

Controlled synthesis and manipulation of ZnO nanorings and nanobows

William L. Hughes and Zhong L. Wang^{a)}

School of Materials Science and Engineering, Georgia Institute of Technology, Atlanta, Georgia 30332-0245

(Received 30 September 2004; accepted 10 November 2004; published online 19 January 2005)

An experimental procedure is presented for the controlled synthesis and manipulation of ZnO nanorings and nanobows at high purity and large yield. Atomic force microscopy manipulation of the nanostructures demonstrates their mechanical toughness and flexibility. Extensive bending of the nanorings and nanobows suggests an extremely high deformation limit with the potential for building ultrasensitive electromechanical coupled nanoscale sensors, transducers, and resonators.

© 2005 American Institute of Physics. [DOI: 10.1063/1.1853514]

Large yield and controlled synthesis of nanostructures are key components for the manufacturing of nanodevices. For nanomaterials, achieving higher purity samples is important for studying their physical and chemical properties. Synthesis of carbon nanotubes with high purity and high yield as well as high designability has, for example, been a very active field.^{1,2} Recently, we have reported the formation mechanism of ZnO nanostructures, including seamless nanorings,³ nanoloops,⁴ nanosprings/nanohelices,⁴ deformation-free nanohelices,⁵ nanospirals,⁶ and nanobows,⁷ which have potential applications as nanoscale electromechanical coupled sensors, transducers, and resonators. These nanostructures are formed by minimizing the electrostatic energy contributed by the spontaneous polarization across the thickness/width of the nanobelt building blocks owing to the unique structure of ZnO. Although the formation process and the growth mechanism have been fully investigated, high-yield synthesis of designed nanostructures remains a challenge. In this letter, we report a synthesis process that produces a high percentage of nanorings and nanobows. This is important progress towards structure control and design for nanostructure synthesis. Using an atomic force microscope, the nanorings and nanobows are manipulated to demonstrate their superior mechanical toughness and flexibility. This is the first group of experiments to show the extreme mechanical deformation of nanorings and nanobows, illustrating their much improved piezoelectric response for electromechanical coupled nanodevices.

Zinc oxide, a key functional material that exhibits semiconductive and piezoelectric properties, has important application in optoelectronics, sensors, transducers, and biomedical applications. ZnO exhibits numerous morphological configurations due to its unique crystal structure and polar surfaces. The nanorings and nanobows under investigation were synthesized by physical evaporation of ZnO powder. Two and a half grams of ZnO powder was used as the source material and placed within the center of a horizontally aligned tube furnace where the temperature, pressure, and evaporation time were manually controlled. Initially, the alumina tube was evacuated to a base pressure of 10^{-2} mbar in order to reduce the oxygen concentration during synthesis. Once the base pressure had been reached, argon was introduced into the alumina tube with a flux of 50 sccm. Argon

was chosen because inert momentum transfer helps purge the alumina tube of oxygen prior to sublimation and helps preferentially grow nanostructures on one side of the alumina tube during ZnO evaporation. The furnace temperature was then raised at $15\text{ }^{\circ}\text{C}/\text{min}$ to $800\text{ }^{\circ}\text{C}$ for 20 min to help form a protective oxide around the resistive coils of the furnace. Once the furnace stabilized at $800\text{ }^{\circ}\text{C}$, the pressure within the alumina tube was raised and maintained at 300 mbar. The furnace was then heated at $\sim 15\text{ }^{\circ}\text{C}/\text{min}$ and maintained at a temperature of $1350\text{ }^{\circ}\text{C}$ for 2 h with a pressure of 300 mbar. During evaporation, the products were deposited onto a catalyst-free polycrystalline substrate that was placed downstream within the alumina tube. Upon termination of the experiment, the pressure within the alumina tube was decreased from 300 mbar to $\sim 10^{-1}$ mbar in 5 s. The deposition temperature for the nanorings/nanobows was estimated to be $\sim 500\text{ }^{\circ}\text{C}$. Once synthesis was complete, the ZnO nanostructures were placed in isopropanol and dispersed onto a (100) silicon wafer for AFM manipulation.

The primary growth directions of ZnO nanobelts are $\langle 0001 \rangle$, $\langle 01\bar{1}0 \rangle$, and $\langle 2\bar{1}\bar{1}0 \rangle$. Their preferred crystallographic orientation will change with variations in temperature and pressure because they are kinetically driven structures. Control over the growth conditions, and therefore the growth direction, will determine the morphology of the synthesized product. Nanobelts dominated by large $\{0001\}$ surfaces have a large spontaneous polarization across their thickness, which are referred to as polar nanobelts, while those dominated by $\{01\bar{1}0\}$ and/or $\{2\bar{1}\bar{1}0\}$ surfaces are called nonpolar nanobelts. We found that experimental differences regarding growing nonpolar nanobelts and polar nanobelts were the temperature ramp rates and the magnitude of the pressure gradients at the termination of synthesis. For example, nonpolar nanobelts were synthesized using a ramp rate of $50\text{ }^{\circ}\text{C}/\text{min}$, a maximum temperature of $1350\text{ }^{\circ}\text{C}$; a gas flow rate of 50 sccm, a pressure of 300 mbar, and a gradual decrease in pressure during natural cooling of the alumina tube. It is important to note that variations in the time at the maximum temperature only change nanostructure size and not nanostructure morphology. In comparison, nanorings/nanobows, which were formed by the polar nanobelts, were synthesized using nearly identical procedures, however, the ramp rate was decreased to $\sim 15\text{ }^{\circ}\text{C}/\text{min}$ and a rapid decrease in pressure was implemented during natural cooling of the synthesis vessel.

^{a)}Electronic mail: zhong.wang@mse.gatech.edu

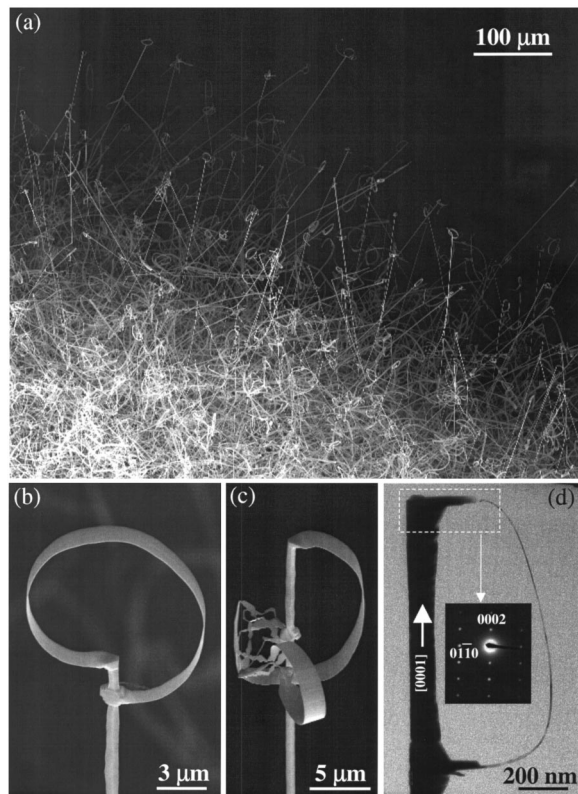


FIG. 1. (a) Large-scale, high-yield and controlled growth of nanorings and nanobows at the tips of ZnO nanorods/nanowires by a sudden change in growth pressure towards the end of the experiment, so that the grow direction switched from $[0001]$ to $[01\bar{1}0]$ or $[2\bar{1}\bar{1}0]$. The polar surface dominated nanobelts bent to form nanorings and nanobows; (b), (c) nanorings and nanobows formed at the tips of the nanowires; (d) TEM image and the corresponding electron diffraction pattern showing the geometry and crystallographic structure of nanobow.

Figure 1 depicts a series of scanning and transmission electron microscopy images, taken along the edge of the alumina substrate, showing the ability of nanobelts to form polar-surface-dominated nanostructures that grow from individual ZnO nanorods. Figure 1(a) shows numerous rings and bows grown from the tips of nanorods. A key observation is that nearly every nanorod has a curly nanoring/nanobow grown from its end. This configuration is created by varying the growth condition as specified above towards the end of the growth process. This is clear evidence of large-yield growth of nanorings and nanobows. Larger magnification SEM images clearly show the potential configurations of nanorings and nanobows grown from the tips of the nanorods [Figs. 1(b) and 1(c)]. The transmission electron microscopy image and corresponding electron diffraction pattern, depicted in Fig. 1(d), shows that the nanorod and nanobow are a single crystal and that the nanorod grows along the $[0001]$ direction. The nanorings and nanobows are formed by rolling the c -plane dominated nanobelts. This process was driven by minimizing the electrostatic energy due to spontaneous polarization across the thickness of the nanobelt.

The polar nanobelts, responsible for the formation of nanorings and nanobows, grow along either the $[2\bar{1}\bar{1}0]$ or $[01\bar{1}0]$ direction. However, a critical point is that the top and bottom surfaces are always the $\{0001\}$ polar surfaces [Fig. 2(a)]. A ring is formed by folding a polar nanobelt so that its c -axis points to the center of the ring [Fig. 2(b)]. A change in

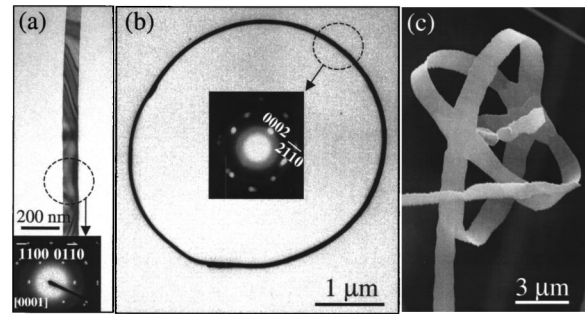


FIG. 2. (a) TEM image of a polar nanobelt growing along $[2\bar{1}\bar{1}0]$; (b) a nanoring formed by self-bending with the c -axis pointing towards the center; (c) SEM image of crossed nanorings originated from the same nanobelt by changing growth direction.

growth direction from $[01\bar{1}0]/[2\bar{1}\bar{1}0]$ to $[10\bar{1}0]/[\bar{1}2\bar{1}0]$ could result in the formation of two crossed rings at 60° angle [Fig. 2(c)].

Manipulation is of critical importance for developing nanostructure-based devices because of the inability to grow one-dimensional nanostructures at site-specific locations with crystallographic-specific orientations. It is therefore the purpose of this study to expand on manipulation techniques that will assist in the fabrication of oscillators and force sensors using the ZnO nanostructures we have synthesized. Previously, transmission electron microscopy and atomic force microscopy have been used to cleave CdO nanobelts and ZnO nanobelts, respectively.^{8,9} As a continuation of the above study, nanorings and nanobows were manipulated using an AFM. However, in contrast to the previous techniques, these nanostructures were systematically deformed rather than intentionally sectioned. Deformation perpendicular to the polar surfaces of ZnO was accomplished by “pushing” the nanostructures parallel to the AFM scanning direction. The contact force was maximized when the nanostructures were pushed (scanned from right to left) and eliminated when pulled (scanned from left to right), or vice versa. In other words, the AFM probe scans continuously and therefore should only contact the substrate and sample when

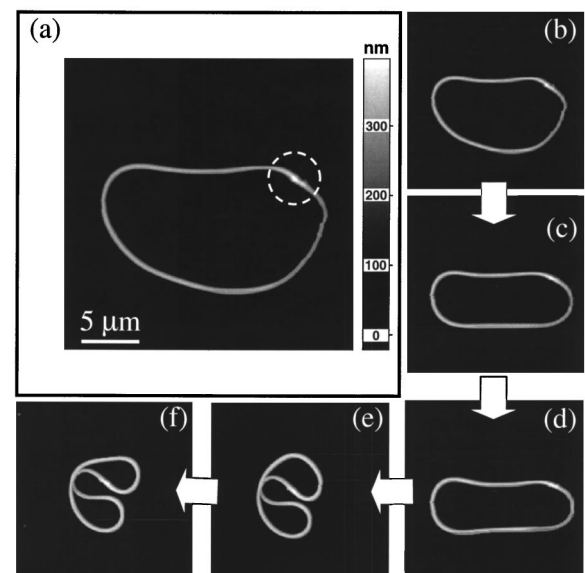


FIG. 3. Series of AFM image showing the manipulation of a single ZnO nanoring into different shapes without causing fracture.

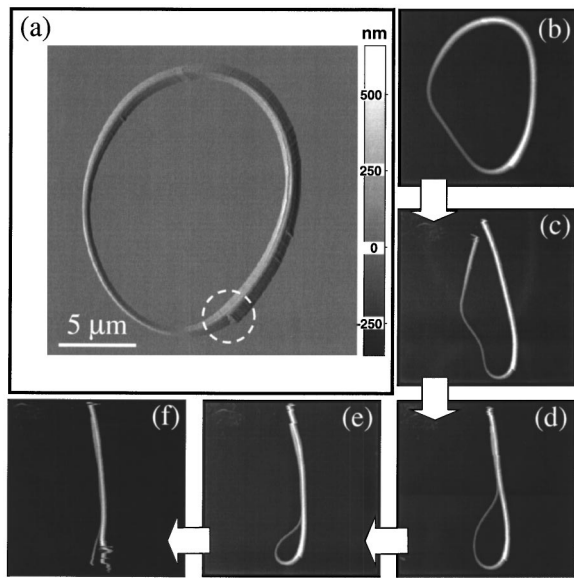


FIG. 4. Series of AFM image showing the manipulation of a single ZnO nanoring by fracturing at one side first and then fracture at the other side at small radius.

scanning in the direction of the desired sample movement. This technique increases manipulation efficiency by eliminating counterproductive movements. The contact force was controlled by modulating the setpoint of the AFM. The nanostructures were firmly attached to the silicon substrate possibly because of capillary forces. The nominal spring constant of the cantilevers used during manipulation was ~ 0.5 N/m.

Figure 3 is an AFM image showing the chemical bond between the two ends of a ZnO polar nanobelt (circle region). The manipulation of the nanoring is shown by a series of AFM images. The corresponding insets below Fig. 3(a) depict the ability of an AFM to stretch a nanoring along its scan direction, as well as its capability to form a kink in the nanoring by pushing from right to left through the imaginary center point of the ring. Remarkably, the nanoring did not fracture during manipulation, although there is an extremely large strain stored within the nanoring.

Figure 4 is an AFM image showing the manipulation of a nanoring. The intent of the experiment was to pull apart the nanostructure at the physical bond (circled region) where the two ends of the nanoring overlapped. During manipulation, the nanoring was made to collapse, upon itself, through a series of pushing and pulling movements. Initially, the nanoring was pushed from the right-hand side and then pulled from the left-hand side [Figs. 4(a) and 4(b)], until it fractured [Fig. 4(c)]. Finally, the remaining loop, shown within Fig. 4(d), was squeezed closed by a series of pulling maneuvers. As depicted in Fig. 4(f), the nanoring fractured for a second time at the point of greatest strain (maximum radius-of-curvature) rather than pulling itself apart at the physical bond.

AFM is an effective technique to position and section ZnO nanostructures. Figure 5 shows a ZnO nanobow that has

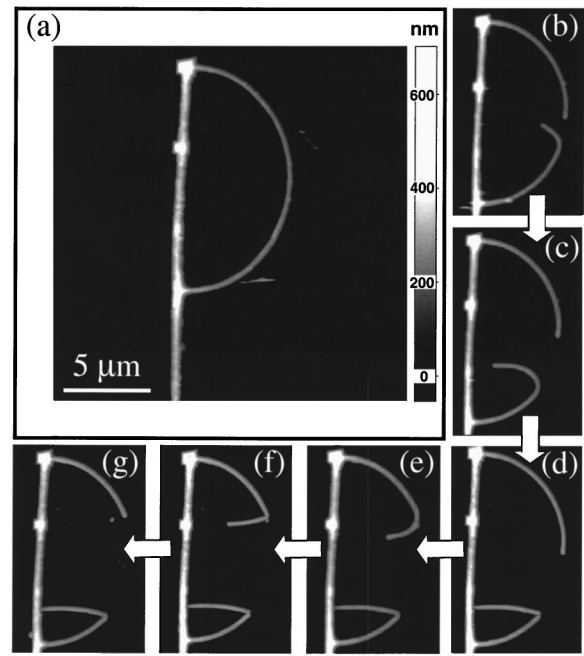


FIG. 5. Series of AFM image showing the manipulation of a single ZnO nanobow into different shapes.

been cut and manipulated using an AFM. One side of the nanobelt was pushed and bent until fracture. Once again, the ability to section and move nanostructures will assist in the formation of nanobelt cantilevers and beams.⁹

In this letter, we have demonstrated a process for synthesis of structurally controlled nanorings and nanobows at a high yield. We found that the pressure changes and/or pressure gradients are responsible for the drastic change in morphology at the end of ZnO nanorods. This sets the foundation to expand the process for producing the nanorings and nanobows at a higher purity. AFM manipulation of the nanorings and nanobows demonstrates their superior mechanical toughness and flexibility, suggesting their extremely high deformation limit with the potential for building ultrasensitive electromechanical-coupled nanoscale sensors, transducers, and resonators.

This work is supported by NSF (DMR-9733160) and NASA Vehicle Systems Program and Department of Defense Research and Engineering (DDR&E).

¹N. R. Franklin, Y. Li, R. J. Chen, A. Javey, and H. Dai, *Appl. Phys. Lett.* **79**, 4571 (2001).

²S. Fan, M. G. Chapline, N. R. Franklin, T. W. Tombler, A. M. Cassell, and H. Dai, *Science* **283**, 512 (1999).

³X. Y. Kong, Y. Ding, R. S. Yang, and Z. L. Wang, *Science* **303**, 1348 (2004).

⁴X. Y. Kong and Z. L. Wang, *Nano Lett.* **3**, 1625 (2003).

⁵R. S. Yang, Y. Ding, and Z. L. Wang, *Nano Lett.* **4**, 1309 (2004).

⁶X. Y. Kong and Z. L. Wang, *Appl. Phys. Lett.* **84**, 975 (2004).

⁷W. L. Hughes and Z. L. Wang, *J. Am. Chem. Soc.* **126**, 6703 (2004).

⁸Z. W. Pan, Z. R. Dai, and Z. L. Wang, *Science* **291**, 1947 (2001).

⁹W. L. Hughes and Z. L. Wang, *Appl. Phys. Lett.* **82**, 2886 (2003).